NRIM SR-95-01

A Simple Geometrical Approach to the Prediction of Plastic Properties of Metal Crystals

by

Ei-ichi FURUBAYASHI

NRIM Special Report
(Research Report)
No. 95–01

1995

National Research Institute for Metals
1–2–1, Sengen, Tsukuba-shi, Ibaraki, Japan

A Simple Geometrical Approach to the Prediction of Plastic Properties of Metal Crystals

by

Ei-ichi FURUBAYASHI

NRIM Special Report
(Research Report)
No. 95-01

1995

National Research Institute for Metals
1-2-1, Sengen, Tsukuba-shi, Ibaraki, Japan

A Simple Geometrical Approach to the Prediction of Plastic Properties of Metal Crystals

by

Ei-ichi FURUBAYASHI

NRIM Special Report
(Research Report)
No. 95–01

Contents

NRIM SR-95–01

A Simple Geometrical Approach to the Prediction of Plastic Properties of Metal Crystals

by

Ei-ichi FURUBAYASHI

Abstract

Methodology has been described, in view of crystal lattice geometry, for deductive prediction of plastic properties of fcc and bcc metal crystals.

The geometrical properties of reciprocal lattice have been used to predict unknown or uncertain properties in one lattice from the known properties in another lattice (this procedure is called *RLC*), since bcc and fcc are in the relation of reciprocal lattice with each other. Probable slip planes and stacking faults in bcc lattice have been predicted from those of fcc metals and compared with experimentally available data in bcc metals. Deformation textures are able to be predicted by the *RLC*, too.

Polarity of shear deformation *(SDP)* on asymmetric crystal planes (as evidenced by well-known polarity in twinning shear) has been treated as the most essential nature in the operation of {112} slip in bcc. The presence of polarity in the critical shear stress for {112} slip in Fe-3%Si alloys was actually found on this basis. The importance of the *SDP* concept has also been proved in the "deformation" associated with γ to α martensitic transformation in ferrous metals. Variant selection phenomena in the martensitic transformation have been interpreted or predicted in this way. Possibility and limitation of such approach have also been described.

Keywords: *crystallography, body centered cubic metals, face centered cubic metals, iron alloys, reciprocal lattice, slip system, twinning system, stacking faults, dislocations, martensitic transformation, variant selection, orientation relation, deformation texture*

1. Introduction

The NRIM (National Research Institute for Metals) Special Report Series has been planned for each volume to publish a collective report prepared by a nominated author. In this consequence, major content will usually be a review on items which have been published in the past. In this volume, new mostly unpublished contents will be described. The article is concerned with the theoretical prediction of uncertain or disputable crystallography of slip systems, martensitic transformation *et al.*, on the basis of the asymmetry of the crystal structure or polarity for deformation in bcc and fcc lattices. The comparison with published experimental data will also be presented.

Crystal geometries for slip, twinning and related dislocation behavior are the first subject of this report. Deformation textures will also be interpreted in relation to the slip behavior. These articles were treated comprehensively in the classical text "Plasticity of Crystals" by E. Schmid and W. Boas(1). The item looks like out of interest for recent researchers, but it will still be essentially important in understanding the mechanical properties of metal crystals. The discussion will be made here to cite recent achievement and to extend further understanding. Martensitic transformation and particularly variant selection phenomena will be treated in a similar way. Many metallurgists, however, have not believed the possibility of either complete understanding or the prediction of plastic properties for actual complicated structures of materials. For this reason, many geometrically evident properties have remained unestablished.

Two simple principles will be presented first in this report, in relation to the geometry of crystal lattices. Published properties which can or cannot be accounted for by these principles will be discussed next. Unknown or uncertain but geometrically expected properties will also be described in view of these principles.

Fundamental crystallographic knowledge which is used in this report has appeared in the texts of physical metallurgy, like those by E. Schmid and W. Boas(1), W.T. Read(2), or C.S. Barrett and T.B. Massalski(3). So, many items are not always sited for each case.

The author is afraid that the contents described will not always be correct, or will make misleading in some respects, and therefore he is expecting to receive information, critical discussions, or helpful suggestions from the readers.

Table 1 Geometrical properties of reciprocal lattice

Standard lattice		Reciprocal lattice
PLANE	⇒	DIRECTION
DIRECTION	⇒	PLANE
Plane normal (Pole)	⇒	Crystal axis
Crystal axis	⇒	Plane normal (Pole)

2. The First Principle: Use of the Geometrical Properties of Reciprocal Lattices

Bcc and fcc lattice structures are mutually in the relation of reciprocal lattice with each other. With this in mind, unknown crystallographic properties of one lattice can be deduced from known properties of another (reciprocal) lattice. Considerable experimental evidence on slip or twinning systems, dislocation Burgers vectors, or other crystallographic properties on plasticity in fcc and bcc metals has been accumulated. For some properties, however, we have to recognize significant lack of reliable experimental data. For example, slip systems in fcc metals has been almost completely evident, but in bcc metals crystallography of slip planes has still been controversial, as will be described in more detail in the following section. Even in such cases, slip systems of bcc metals can be deduced from those of fcc metals, based on the fact that the bcc is the reciprocal lattice of fcc.

The useful properties of reciprocal lattice are as follows; a certain direction [hkl] and plane (uvw) in a (standard) lattice are transformed into the same index plane (hkl) and direction [uvw] respectively in the reciprocal lattice, as summarized in Table 1. As a result, a shearing system, *i.e.* a combination of direction [hkl] and plane (uvw), in the standard lattice is transformed to a new shearing system [uvw](hkl) in the reciprocal lattice. This kind of exchange relation between the plane and the direction will be called as *"RLC (Reciprocal Lattice Correspondence)"* hereafter.

3. The Second Principle: Asymmetry of Plane Stacking and Polarity of Shear Direction

Most of lattice planes in crystals have *"asymmetry"* with respect to their stacking direction, or have no mirror reflection symmetry. For example, {111} planes in fcc lattice have three cyclic layers of stacking; ABCABC in one direction, while CBACBA stacking in the reverse

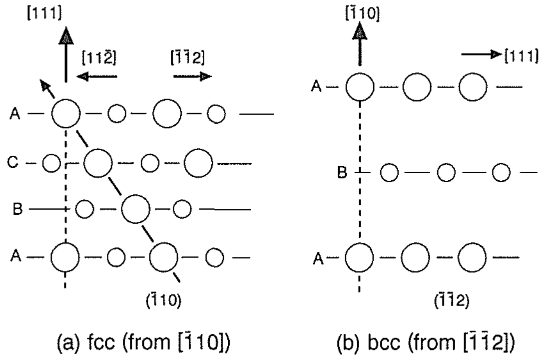

(a) fcc (from [$\bar{1}10$]) (b) bcc (from [$\bar{1}\bar{1}2$])

Fig. 1 Stacking of atomic layers of close-packed planes viewed from perpendicular directions. Large circles show the atoms on a plane on the drawing, and small circles are those on the next plane. (a) Asymmetric stacking of (111) plane stacking in fcc lattice structure viewed from [$\bar{1}10$]. (b) Symmetric ($1\bar{1}0$) plane stacking in bcc lattice structure viewed from [$\bar{1}\bar{1}2$].

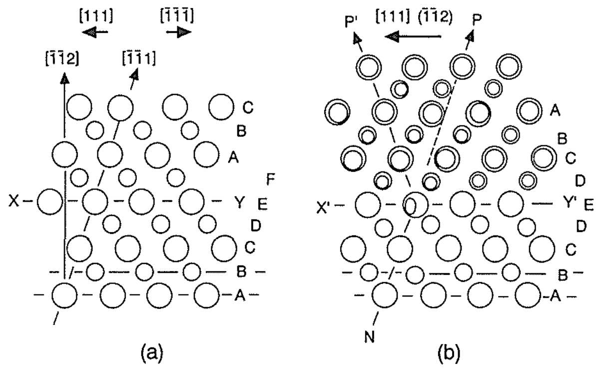

Fig. 2 Schematic view of polarity of twinning shear [111]($\bar{1}\bar{1}2$) in bcc lattice viewed from [$\bar{1}10$] direction. Large circles show the atoms on a plane on the drawing, and small circles are those on the next plane. (a) Atom arrays in (untwinned) fcc lattice, showing six layers stacking of ($\bar{1}\bar{1}2$) planes ABCDEF which are perpendicular to the sheet and are horizontal (i.e. parallel to X-Y). (b) The same arrays in twinned lattice; the twin boundary lies along X′-Y′. Double circles indicate the atoms in the twinned crystal.

direction as shown in Fig. 1(a), thus having asymmetry. On the other hand, {011} type planes in bcc lattice have ABAB stacking which has mirror reflection symmetry, as shown in Fig. 1(b). {001} type planes in fcc or bcc lattice will be another example of symmetry, but most planes are of asymmetry.

In general, shear deformation along such asymmetric planes have *"polarity."* For example, shearing along [$11\bar{2}$] direction on (111) plane (hereafter described as [$11\bar{2}$](111)) in fcc lattice is not crystallographically identical with the opposite [$\bar{1}\bar{1}2$](111), thus having polarity as shown in Fig. 1(a). But [$\bar{1}10$](111) has not polarity where [$\bar{1}10$] is perpendicular to the figure. Every direction having such polarity (*e.g.* [$11\bar{2}$]) has to be normal to an asymmetrically stacked plane (*i.e.* ($11\bar{2}$) in this example), and this will be another expression for the direction to have polarity.

Many intrinsic mechanical properties of metals and alloys originate from the polarity of shear described here.

Table 2 Reciprocal lattice correspondence *(RLC)* between FCC and BCC lattices for the elements of slip, twinning and stacking faults.

FCC lattice		BCC lattice	
Slip plane:	□ {111}	Slip directions (burgers vectors)	□ <111>
	△ {001}		○ <001>
Slip directions (burgers vectors)	□ <011>	Slip planes:	△ {011} △ {112}
Slip directions (partial dislocation burgers vector)	□ <112>		?? {123} ?? Non crystallographic {hkl}
Twinning plane:	□ {111}	Twinning shear direction:	□ <111>
Twinning shear direction:	□ <112>	Twinning plane:	□ {112}
Stacking fault plane:	□ {111}	Burgers vector of partials	◎ <111>
Burgers vector of partials	□ <112>	Stacking fault:	◎ {112}

□: Experimentally established facts
△: Evidence is limited
◎: Not evidenced directly but geometrically probable
○: Geometrically possible in limited cases
??: Documented so far but geometrically improbable

And therefore the polarity will be a useful point of view in analyzing or predicting the properties. Stacking faults*(SF)* and twins will be formed on the planes of asymmetric stacking, as discussed later. Actually in fcc metals, these are formed on {111} planes, as shown in Table 2. As shown in Fig. 2, mechanical twinning in bcc metals takes place on {112} planes having ABCDEF type (six layers) stacking, and twins are formed by $[111](\bar{1}\bar{1}2)$ shear (called *twinning shear*) forming ABCDEDCBA... type stacking, so that the atom array NOP in Fig. 2(b) along $[\bar{1}\bar{1}1]$ is transformed to a deflected array NOP′. But twins are not formed by $[\bar{1}\bar{1}\bar{1}](\bar{1}\bar{1}2)$ or $[111](11\bar{2})$ shear (called *antitwinning shear*), thus having polarity.

Martensitic transformation (MT) is a phenomenon similar to deformation; the "deformation" can be defined as a kind of MT in which the original lattice is transformed into the same lattice, whereas in MT the lattice is transformed into a different lattice. MT from fcc to bcc (or bct) lattices is associated with some shear deformations. In understanding the mechanism of MT, one of the most important aspects is believed to be the presence of polarity in the shear deformation. Examples will be shown as follows. Crystallographic orientation relations between martensite and matrix have been described in terms of the *Phenomenological Theories*(4). In the theories, *Lattice deformation*, as suggested by E.C. Bain(5) and is called *"Bain strain,"* is treated as the principal operator in the mathematical formula of MT from γ to α in ferrous alloys, *i.e.* ~20% compression along one of the cubic axis (Z) and ~12% elongation along perpendicular (X and Y) axes of austenite lattice, as shown in Fig. 3. Therefore the *Bain strain* has polarity in view of the "deformation" of austenite. The double shear mechanism of γ to α MT by J.S. Bogers and W.G. Burgers(6) will also be said to have polarity, since the first shear in the mechanism is parallel to the twinning shear *i.e.* along $[11\bar{2}]$ twinning direction on (111) plane in fcc lattice. Significance for this will be described in the later section.

The author will call such polarity associated with asymmetrical plane stacking as *"SDP (Shear Deformation Polarity)"* hereafter.

Several examples of applications, in which useful information would be drawn from the *RLC* and *SDP*, will be shown in the next section.

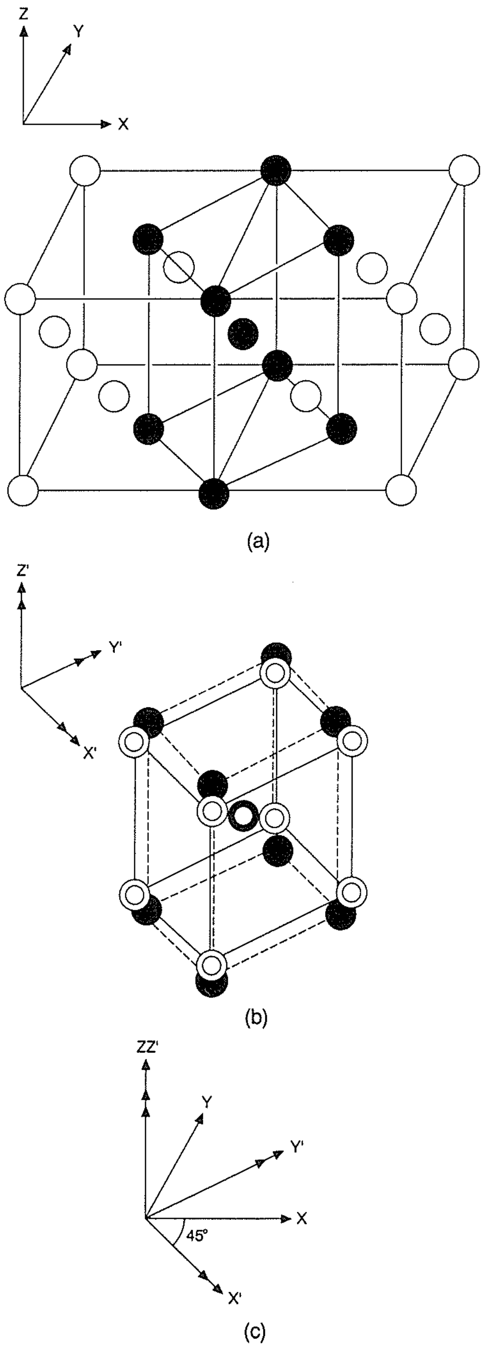

Fig. 3 Interrelation between the lattice deformation *(e.g. Bain strain)* and the *Bain* orientation relation in γ to α martensitic transformation in steel. (a) Hypothetical body centered tetragonal lattice (●) in normal γ (fcc) lattice (○). (b) Formation of α (bcc) lattice (◎) due to the lattice deformation from the hypothetical bct lattice (●). (c) Orientation relationship between γ and α lattices.

4. Applications of the Principles to Predict Uncertain Plastic Properties

In this section, several disputable plastic properties of bcc metals will be discussed in view of the *SDP* and/or *RLC* principle described above.

4.1 Slip Systems in BCC Metals

In fcc lattice, crystallography of slip deformation has been well established so far. As shown in Table 2, slip planes and directions are {111} and <011>, respectively. {001} type slip plane (*i.e.* <110>{001} type slip system) is also operative but is exceptional, as will be described later. In bcc metals, however, slip plane geometry is not always evident, though the slip direction (*i.e.* the direction of Burgers vector (BV)) is definitely <111>. More precisely, the slip planes have been considered to be {011}, {112}, {123} or higher indices planes or even noncrystallographic ("banal slip") planes(1, 3). The limiting condition which is geometrically available is that the zone axes of the slip planes are parallel to the slip direction <111>; the situation is called "pencil glide."

4.1.1. Experimental evidence

Such crystallographic uncertainty of the slip planes in bcc metals is due to much wavy nature of slip traces observed metallographically on deformed crystal surfaces, as compared to fcc metals.

Besides the slip trace analysis, the orientation change (*i.e.* rotation of orientation) of crystals, or the asterism of diffraction spots due to deformation have been examined by X-ray diffraction methods(1, 3, 7, 8). Generally speaking, however, the asterism will be an indication of lattice curvatures which are formed by dislocations remaining in the crystal. In view of finding the operative slip elements, information is necessary on the dislocations which have passed through and gone out of the crystal. The rotation of orientation will meet the requirement, but in conventional tensile testing, the slip direction can only be identified by the stress axis rotation, but no information is available on the slip plane(1). As a result, either the asterism or the axis rotation measurement by X-ray diffraction is not an effective means for the determination of the slip planes. Exemplary experimental results for the slip system determination in bcc metals and alloys are as follows. C.S. Barrett *et al.*(9) stated "Slip in iron is on {011}, {112} and {123} planes at all temperatures investigated (between 77 K and 810 K), but in iron silicon alloys low deformation temperatures or silicon contents higher than ~4 mass% (hereafter denoted as "%") cause slip to be confined on {011} planes." This result will suggest that the {011} planes are the most substantial slip planes in bcc lattice.

Actually, R. Maddin *et al.* proposed on the basis of observations by Mo(7) or Nb(8) that the {011} is the only elemental slip planes, and that wavy slip traces would be a result of statistical choice among non-parallel {011} elemental slip planes. This view will be called *"elemental slip criteria"* hereafter.

Detailed optical microscope studies in NRIM, for several substitutional iron alloy single crystals have shown that the slip traces are not always parallel to crystallographic planes with low Mirrer indices(10–12). This is not surprising because such slip traces are the intersections of slip bands (*i.e.* deformed region which many dislocations passed through) with the crystal surfaces. Since the slip bands have some width, the band traces are not always parallel to the slip traces of individual dislocations. Even with direct observations of slip trace of individual dislocations in Fe-3%Si(13) or in Nb(14), either view of the *elemental slip criteria* or the crystallographic slip on low indices planes is not supported by *in situ* deformation in a high voltage transmission electron microscope (TEM). Slip traces of individual dislocations in a slip band were nearly parallel but not exactly parallel to the band trace(13).

4.1.2. Geometrical prediction

In this way, it is not possible experimentally to get more detailed crystallographic view of the slip plane geometry at present. So, application of the *RLC* principle has been tried to make assure probable slip planes in bcc lattice from established crystallography of slip systems in fcc lattice, as shown below.

Table 2 shows predicted elements of twinning, stacking faults and slip which have not always been established in bcc. Experimentally established facts in fcc lattice (which are also shown in Table 2), are the basis for the prediction in bcc lattice.

Slip planes in bcc is considered to be identical to the slip direction in fcc according to the *RLC*. First of all,

Table 3 Slip geometries and b/d for total dislocations in BCC or FCC lattice.

Lattice	Burgers Vector BV	|BV| = b	Slip plane {hkl}	Slip plane spacing (d)	b/d
BCC	a/2<111>	$\sqrt{3}a/2$	{011}	$a/\sqrt{2}$	1.225
	a <100>	a	{011}	$a/\sqrt{2}$	1.414
	a/2<111>	$\sqrt{3}a/2$	{112}	$a/\sqrt{6}$	2.121
	a/2<111>	$\sqrt{3}a/2$	{123}	$a/\sqrt{14}$	3.240
FCC	a/2<011>	$a/\sqrt{2}$	{111}	$a/\sqrt{3}$	1.225
	a/2<011>	$a/\sqrt{2}$	{100}	a	1.414

Table 4 Slip geometries and b/d for partial dislocations in BCC or FCC Lattice.

Lattice	Burgers Vector BV	|BV| = b	Slip Plane {hkl}	Slip plane spacing (d)	b/d
BCC	a/6<111>	$\sqrt{3}a/6$	{112}	$a/\sqrt{6}$	0.707
	a/8<011>	$\sqrt{2}a/8$	{011}	$a/\sqrt{2}$	0.250
	a/4<211>	$\sqrt{6}a/4$	{011}	$a/\sqrt{2}$	0.866
FCC	a/6<112>	$a/\sqrt{6}$	{111}	$a/\sqrt{3}$	0.707

<011> and <112> are the slip directions in fcc lattice, since the former and the latter are parallel to the BV of total and partial dislocations, respectively. But <123> or other directions of higher indices can not be the slip direction in fcc lattice. From these facts it may be concluded that {011} and {112} planes are probable slip planes in bcc lattice, but the planes of {123} or of higher indices are improbable.

In the second place, slip on {001} planes has been observed in aluminium in limited conditions(15, 16) like high temperatures. According to the *RLC*, slip along <001> direction can have reality in bcc lattice, as *predicted from the operation of the {001} slip plane in* fcc. Since no experimental evidence had been provided for the <001> slip operation in bcc metals, an experimental trial for the confirmation was performed at NRIM by Shin Takeuchi(17) but was not successful. On the other hand, in *an ordered bcc lattice, i.e.* CsCl type (B1) structure, <001> slip is known to operate as well as <111> slip, depending on the bonding nature being nonmetallic or metallic(18). For example, in intermetallic NiAl crystal <001> is the major operative slip directions, but in FeAl <111> slip is mainly operative. This will be another evidence for the hard operation of <001> slip in (disordered) bcc structure, because the ordering makes the operation of conventional <111> slip more difficult, since the slip disturbs the ordered lattice, while <001> slip does not.

Besides these, <001> dislocations are considered to have high Peierls stress, as shown below. Table 3 shows the geometrical parameters of total dislocations in bcc and fcc lattices. The Peierls stress for dislocations is estimated by equation (1) as a function of a parameter (b/d), where b and d are the size of the Burgers vector and slip plane spacing, respectively. Other parameters, σ_p, G and υ are Peierls stress, shear modulus and Poison's ratio, respectively.

$$\sigma_p = \left[\frac{2G}{(1-\upsilon)}\right]\exp\left[\frac{-2\pi d}{b(1-\upsilon)}\right] \cdots\cdots\cdots\cdots\cdots\cdots \quad (1)$$

Therefore, <001> slip seems rather hard to operate than <111> slip in bcc lattice. Thirdly, the activity of <111> slip for different planes is also suggested from Table 3; as far as the total dislocations in bcc are concerned, slip planes other than {011} are not operative in view of the high Peierls stresses (high b/d values). However, the situation will be modified when the dislocations are extended. Table 4 shows partial dislocations have much lower values of b/d than total dislocations. This will be a reason which, in spite of the loss of energy due to stacking fault formation, makes possible for the operation of slip on {112} plane on which dislocations are considered to be extended in bcc lattice (see 4.4).

4.2 Deformation Textures

The deformation texture, *i.e.* preferred orientation distribution developed by plastic deformation, is the next subject of applying the *RLC*. Since the deformation texture is correlated with the deformation by slip, the same kinds of discussion in 4.1 will be applicable. In case of uniaxial deformation, simple formulation is possible. For example, in case of tensile or compressive deformation under single slip operation, there is a general tendency that

a.) the tensile direction rotates to the operative slip direction, and

b.) the compression direction rotates to the slip plane normal(1, 19, 20).

Table 5 Uniaxial deformation textures

Deformation mode (reference axis for texture presentation)	Textures in FCC		Textures in BCC	
		Reference		Reference
TENSION (parallel to the axis)	<111>	(19)	<011>	(20)
	<112>	(19)		
DRAWING (parallel to the axis of wires)	<111>	(1), (3)	<011>	(1), (3)
	<001>	(1), (3)		
COMPRESSION (parallel to the axis)	<011>	(1), (3)	<111>	(1), (3)
			<112>	(20)
			<001>	(3), (20)
TORSION (parallel to the longitudinal direction)	<111>	(1)	<011>	(1)
			<112>	(1)

But in practice, experimental texture data for tension textures are not available, because it is difficult to deform by tension to such large strains that deformation textures would be developed. The rotation of orientation in single crystals can be used to estimate the tensile texture instead. Drawing textures are available to simulate the tensile deformation too, though the stress states in drawing is more complicated than in tensile deformation. As far as the plastic strain is concerned, drawing is nearly equivalent to tensile deformation.

Torsional deformation will also provide a texture in which slip plane tends to rotate to become parallel to the plane of maximum shear stress (*i.e.* the plane normal to the specimen axis). Table 5 shows the textures developed under such uniaxial deformation modes. From Table 5 one will find the *RLC* principle is valid; crystallographic parallel relation exists between tensile (or drawing) textures in fcc and compression textures in bcc, or *vice versa.*

The *RLC* principle also holds in biaxial rolling textures, as shown in Table 6, one will look at the parallel relation between rolling direction in fcc and rolling plane normals in bcc, and *vice versa.* In actual rolling deformation, three dimensional internal stresses⁽²¹⁾ and multiple operation of slip systems are involved. In appearance, however, rolling textures consist of a combination of tensile texture along the rolling direction, and compression texture along the rolling plane normal. This will be due to the fact that there are some geometrical limiting conditions in selecting the operative slip systems in rolling; the conditions will be similar to the above mentioned principles (a) and (b) for uniaxial case.

Table 6 Rolling (biaxial) textures

FCC		BCC		Reference
Parallel to the rolling				
Direction	Plane	Direction	Plane	
<112>	{110}			(1)
<111>	{112}			(1)
<001>	{110}			(66), (3)
		<110>	{001}	(1)
		<110>	{112}	(67), (3)
		<112>	{111}	(67), (3)

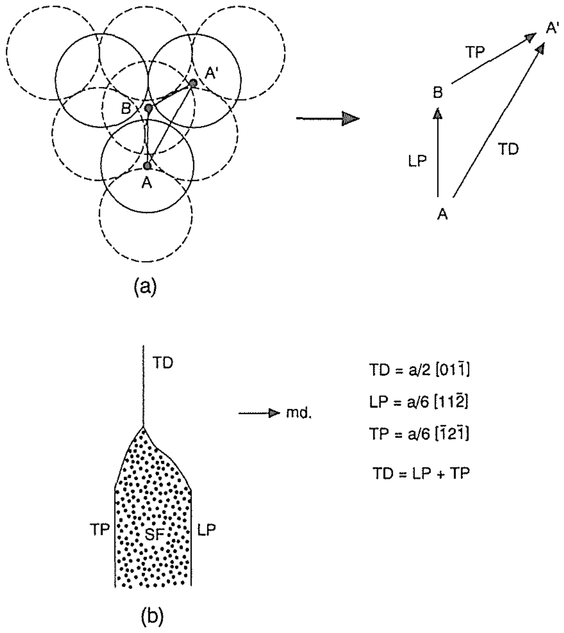

Fig. 4 Drawings showing the relation among atomic stacking structure of an extended dislocation accompanied with a stacking fault (SF) in fcc lattice, and Burgers vectors for total dislocations (*TD*) and for (leading or trailing) partial dislocations (*LP* or *TP*, respectively).

4.3 Polarity in Slip in FCC and BCC Metals

The polarity of slip deformation in fcc lattice will be described first. According to the *SDP* principle, <112>{111} slip system in fcc has polarity but <011>{111} slip system not. In other words, the polarity exists in partial dislocations but not in total dislocations. The polarity in partial dislocations will now be described in detail. It is wellknown⁽²⁾ that *total* (perfect) *dislocation* (*TD*, having Burgers vector BV = a/2[01$\bar{1}$]) in fcc lattice is divided into two *Shockley partial* (incomplete) *dislocations* (having BV = a/6[11$\bar{2}$] and a/6[$\bar{1}$2$\bar{1}$]), and a piece of

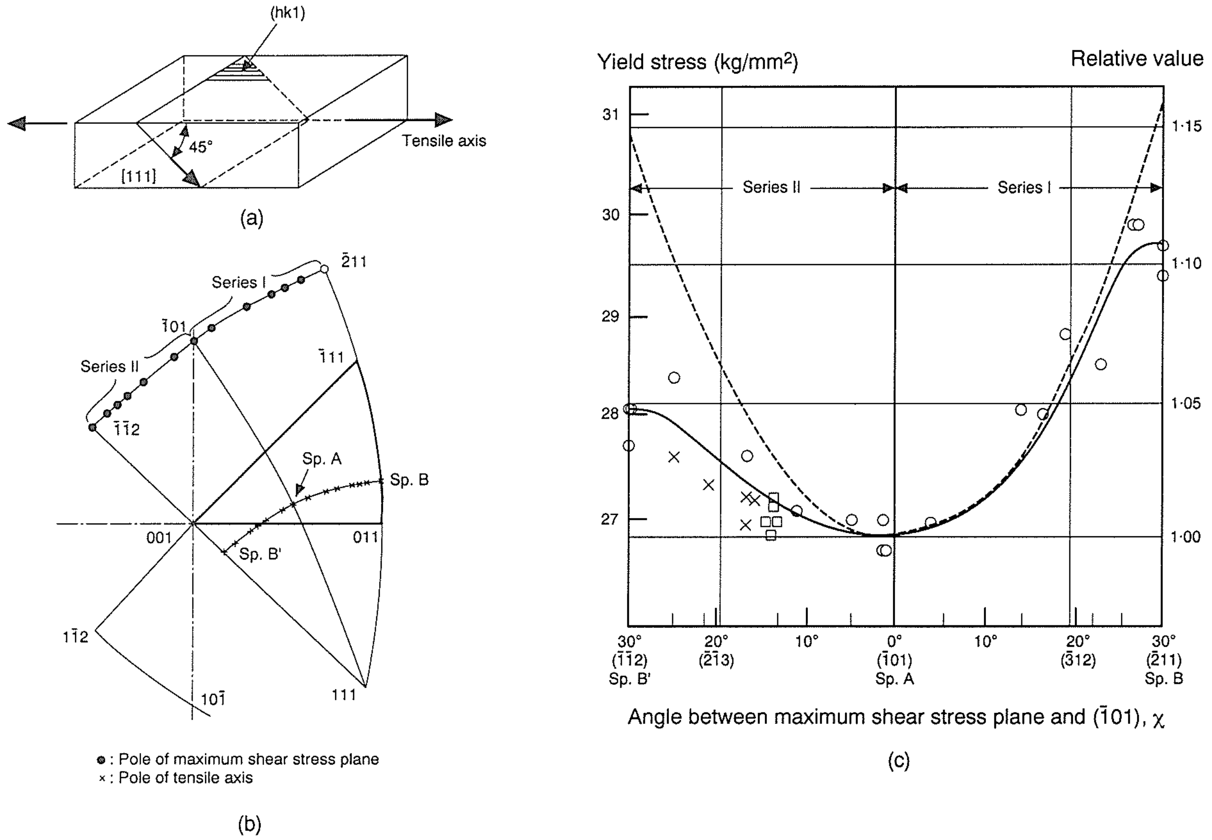

Fig. 5 The first experimental data showing the polarity in {112} slip in bcc transition metal of iron by T. Taoka *et al.*(10). (a) and (b) Tensile orientations of Fe-3 mass%Si single crystals investigated, and (c) Orientation dependence of yield stress at room temperature. Marks ○ and × indicate values for [111] and [111], respectively. Marks ☐ are replots of the abscissa of × by regarding the slip direction as [111].

stacking fault *(SF)* ribbon is formed between the two partials, as shown in equation (2) and in Fig. 4.

$$\frac{a}{2}[01\bar{1}] = \frac{a}{6}[11\bar{2}] + \frac{a}{6}[\bar{1}2\bar{1}] \quad \cdots\cdots\cdots\cdots \quad (2)$$

In the absence of applied stress, the distance between the partials or the width of SF ribbon is inversely dependent to the SF energy. In the presence of applied stress, the two partials are called as *"leading partial (LP)"* and *"trailing partial (TP)"* respectively, depending on the migration direction (md.). SF extends only when the resolved shear stress for *LP* is larger than that for *TP*. In other words, SF extends if the *LP* and *TP* are the twinning partial (*e.g.* AB or A'B in Fig. 4) and antitwinning partial (*e.g.* BA or BA'), respectively. These are the mechanism of polarity in <112>{111} slip in fcc lattice.

In bcc lattice, polarity is expected in any <111>{hkl} slip system except <111>{011} by the *SDP* principle. As described in section 4.1, however, slip planes other than {011} and {112} are not present. Therefore, <111>{112} is the only slip system of having polarity.

Experimental evidence for the polarity of slip in bcc was known on β brass or alkali metals from the early times, but not in bcc transition metals until 1964, at which strength polarity in an iron alloy was found by T. Taoka *et al.* at NRIM(10). This was the result of an experimental work which was designed to confirm the simple prediction that twinning shear would cause slip polarity in <111>{112} slip of Fe-3% Si alloy(10, 11). Figure 5 shows an example of the data by T. Taoka *et al.*(10). Tensile stress was applied to the single crystals of various orientations shown in Fig. 5(b). The orientation dependence of yield stress is shown by solid line in Fig. 5(c). When the operative slip system is confined only

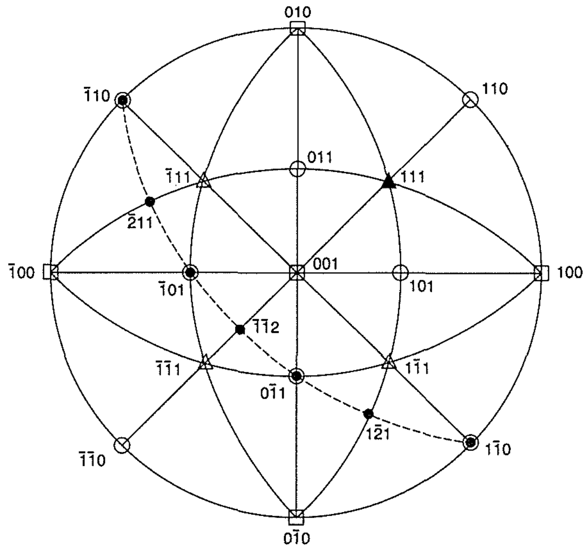

Fig. 6 Standard stereographic projection of reference orientations used in this report for cubic crystals.

to $[111](\bar{1}01)$, the expected orientation dependence of yield stress will be shown by dash line. The actual yield stresses of Sp.B and B′ are lower than the dash line, and this means the slip operation on {112} type planes is easier than on {011} planes in "Sp.B" or "Sp.B′". This will provide a positive evidence for the physical reality of the {112} slip. Another point to be noted is that the yield stress of Sp.B′ oriented to have twinning shear is evidently lower than that of sp.B oriented for antitwinning shear. The presence of the slip polarity in the operation of the <111>{112} system is thus proved.

At that time B. Sestak *et al.*(22) found the difference of yield stress in Fe-Si alloy single crystals between tension and compression mode of deformation, but they attributed the difference to the normal stress effect. The explanation by Sestak *et al.* seemed incorrect and later their results were proved to be due to the slip polarity(10, 11).

After the discovery, similar slip polarity was found in many other bcc transition metals of Nb(23, 24), Ta(25), Mo(25, 26) and W(27). Since then, the significance of the polarity of slip has been recognized as an evidence for the asymmetric structures of dislocation core in bcc metals. Many computer simulation studies on the dislocation core structures and Peierls stress calculation in bcc lattice have been made on this basis, as reviewed by P.B. Hirsch(28) or J.W. Christian(29).

4.4 Mechanical Twins and Stacking Faults in FCC and BCC Metals

In both cases of bcc and fcc metals, mechanical twinning occurs when the applied stress has maximum resolved stress on the twinning shear (as shown before), but does not on the antitwinning shear(30). This fact is well recognized in bcc metals in which mechanical twinning is a proper mode of deformation. However in fcc metals, mechanical twinning is harder to occur than in bcc metals. In fcc pure metals twinning does not occur except at cryogenic temperatures(32, 33), but in alloys twinning is a mode of deformation under wider conditions(33). The twinning is active at early stages of deformation in bcc metals and it is reduced by slip operation, but it continues to higher strains in fcc alloys(30, 31, 33). When the stress of twinning shear is applied to fcc metals, the SF ribbon between the leading and trailing partials is made extended. In other words, the same sense of polarity exists between twinning and SF formation.

The extended dislocation in fcc is composed of two partial dislocations and a piece of SF between them. The SF is composed of two atomic layers of fault, which is regarded locally to be hcp lattice. From this, it will be said, in general, that SF is a kind of defects which, firstly, provide local atomic displacement similar to the phase transformation, and, secondly, are surrounded by partial (incomplete) dislocations. As will be shown later, there exist some cases in which incomplete dislocations are not always twinning dislocations.

The possibility of the SF in bcc metals has been the matter of controversy, and the reality has not been established yet. Though there exist some experimental observations of SF in bcc by TEM, the evidence has been confined to unalloyed niobium(34, 35). This has made one to consider as due to some artifacts, since Nb has high solubility of hydrogen or other interstitial elements, and it has large tendency for the impurity absorption during the specimen preparation.

According to the analogy to fcc metals, the most probable SF in bcc metals will form on the twinning planes, with a shearing along the twinning directions, as has been proposed previously(36, 37). This type of SF will be called as *"Twin-type"SF* hereafter. The stacking of {112} plane in bcc is six holds, as seen in Fig. 2(a). The shear system of the SF will be the same as that in

Table 7 Mirror indices of the "twinning planes" in the CSL Model; *i.e.* the planes on which most densely packed coincident sites are located (after D.G. Brandon(42))

Σ	Twinning Plane	
	FCC	BCC
3	{111}	{112}
5	{012}	{013}
7	{123}	{123}
9	{122}	{114}
11	{113}	{233}
13a	{023}	{015}
13b	{134}	{134}
15	{125}	{125}
17a	{014}	{035}
17b	{223}	{334}

twinning; a/6<111>{112} in this case, as described by the first right term of equation (3).

$$\frac{a}{2}[111](\bar{1}\bar{1}2)=\frac{a}{6}[111](\bar{1}\bar{1}2)+\frac{a}{3}[111](\bar{1}\bar{1}2) \qquad (3)$$

This concept for SF in bcc is coincident with the prediction by the *RLC*, as already shown in Table 2.

However, since bcc is not a close packed structure, the SF energy will be very high essentially irrespective of the planes on which the SF lies. Therefore the width of extended dislocations will be invisible by means of TEM. According to H. Suzuki, the SF energy on {112} plane of bcc iron is estimated to be ~950 mJ/m^2, and resulting distance between partial dislocations would be smaller than **b**(37).

Besides the SF on {112} plane, several theoretical possibilities of SF in bcc have been proposed on *e.g.* {011}(38, 39) or {013}(35, 40) plane, but there is no direct experimental evidence to date. Among them, SF on {013} will be geometrically possible by the *SDP* since the stacking of {013} plane is asymmetrical. Evidence of twinning on the {013} plane(41) will also support the possibility for SF on the {013}. Further possibility of the Twin-type SF will be suggested; *i.e.* SF on the "twinning" planes other than Σ 3 appearing in the Coincident Site Lattice (CSL) model(42), *e.g.* {012}, {123} *etc.* in fcc and {013}, {123} *etc.* in bcc, as shown in Table 7. Since annealing twins of Σ 11, Σ 9, Σ 17 or Σ 13 type have been identified in fcc metals of copper and Fe-Ni alloy(43), the possibility for the SF on these "twinning" planes in bcc can not be neglected at present, though such SF seems improbable.

On the other hand, Twin-type SF on symmetric {011} plane will be impossible by the *SDP* principle. However, J.B. Cohen *et al.*(39) proposed a model suggesting the SF other than twin type SF in bcc; that is, extended dislocation on {011} plane would consist of three partial dislocations, as shown in equation (4).

$$\frac{a}{2}[111]=\frac{a}{8}[011]+\frac{a}{4}[211]+\frac{a}{8}[011] \;\ldots\ldots\ldots\ldots \qquad (4)$$

The SF in this case is composed of three atomic layers, and among them two types of faults are involved. Each of the three faults makes the bcc lattice into deformed fcc or hcp lattice.

4.5 Polarity of Shear in Martensitic Transformation and Variant Selection

The theoretical formulation of crystallography of the martensitic transformation (MT) has been provided by M.S. Wechsler *et al.*(44) or by J.S. Bowles and J.K. Mackenzie(45) in terms of the matrix algebra. These "Phenomenological Theories" have provided very accurate description of the observed crystallographic relations between the lattices before and after MT, but the accuracy does not always help us to construct kinematic mechanisms of transformation. For example, it is not possible even briefly to predict a variety of orientations of transformation products (due to variant selection) with the theories.

Among many properties associated with MT, the variant selection will be one of the most realistic properties, because it can be analyzed from the experimentally available data of orientations. But the analyses of observed orientations or textures by existing variant selection models were not successful, until new models with experimental support were proposed by Y. Higo *et al.*(46), M. Kato and T. Mori(47) and E. Furubayashi *et al.*(48–50), and H. Miyaji *et al.*(51, 52). This is because in unsuccessful models, we believe, the polarity has not been taken into account in the "deformation" associated with MT. The polarity is the most essential nature in the variant selection phenomena and probably in the transformation mechanism itself.

Table 8 Orientation relations for martensitic transformation from γ to α in ferrous alloys.

Title of relation	Lattice Correspondence	Mutual orientation difference in martensite Δ θ (deg)		
		Referring to *Bain*	Referring to *N*	Referring to *K-S*
Bain	$\{001\}_{\gamma}$ // $\{001\}_{\alpha}$ $<100>_{\gamma}$ // $<110>_{\alpha}$	0	9.74	11.06
N	$\{\{111\}_{\gamma}$ // $\{011\}_{\alpha}$ $<11\bar{2}>_{\gamma}$ // $<01\bar{1}>_{\alpha}$	9.74	0	5.26
K-S	$\{111\}_{\gamma}$ // $\{011\}_{\alpha}$ $<01\bar{1}>_{\gamma}$ // $<11\bar{1}>_{\alpha}$	11.06	5.26	0
Pitsch	$\{100\}_{\gamma}$ // $\{01\bar{1}\}_{\alpha}$ $<01\bar{1}>_{\gamma}$ // $<11\bar{1}>_{\alpha}$	9.74	~8	5.26

Table 9 Crystallographic concepts involved in orientation relations or lattice correspondence in γ to α transformation in ferrous alloys.

Title of relation	Lattice correspondence	Concepts involved	Polar-ity
Bain	$\{001\}_{\gamma}$ // $\{001\}_{\alpha}$ $<100>_{\gamma}$ // $<110>_{\alpha}$	Bain strain	○
N	$\{111\}_{\gamma}$ // $\{011\}_{\alpha}$	Parallelism of closest-packed planes	?
	$<11\bar{2}>_{\gamma}$ // $<01\bar{1}>_{\alpha}$	?	
K-S	$\{111\}_{\gamma}$ // $\{011\}_{\alpha}$	Parallelism of closest-packed planes	×
	$<01\bar{1}>_{\gamma}$ // $<11\bar{1}>_{\alpha}$	Parallelism of nearest atom direction	
Pitsch	$\{100\}_{\gamma}$ // $\{01\bar{1}\}_{\alpha}$	Parallelism of close-packed planes	×
	$<01\bar{1}>_{\gamma}$ // $<11\bar{1}>_{\alpha}$	Parallelism of nearest atom direction	

As described below, the range of orientation distribution of transformation products does not change virtually with or without variant selection if one apply the models without polarity. The lack of the polarity concept seems to be a cause of confusion in the variant selection analysis, as described below.

4.5.1. The orientation relationship as a formulation of transformation mechanism

For the MT in ferrous alloy systems, *Kurdjumov-Sachs (K-S)*(53), *Nishiyama (N)*(54), *Pitsch*(55), and *Greninger-Troiano (G-T)*(56) besides the *Bain*(5) are known as the orientation relation or the lattice correspondence, as shown in Table 8.

As will be seen in the table, orientation differences among these relations are very small. Each orientation of the variants in *K-S et al.* is distributed around the orientation of *Bain* variants(49, 53). Experimental accuracy of orientation determination by early works with the X-ray diffraction method(53, 54) seems insufficient in distinguishing each of the relation. This is because the orientation distribution in the cross section of incident X-ray beam was so large that the diffraction spots came from many transformed crystals. Even with the recent diffractometer methods, the situation will not be improved. The use of the electron diffraction(55, 56) is worthy to note in view of the small beam size, but will make another inaccuracy problem due to theoretical uncertainty in the place-orientation determination(57), and has been pointed out as insufficient to distinguish them(58).

Therefore, these orientation relations (i.e. *K-S, N, Pitsch*, as well as *Bain*) should be of conceptional or theoretical meanings, rather than experimental evidence. For this meaning, we are going to discuss the theoretical concepts involved in these relations. The *G-T* relation will not be discussed, because this does not seem to be other than an experimental relation.

Table 9 shows the concepts involved in the orientation relations in MT from fcc to bcc lattice. In this table, the *Bain* relation has polarity as mentioned earlier, but *K-S* or *Pitsch* relation does not have polarity because of the *SDP* principle. The concepts involved in *N* relation is not clear.

4.5.2. Variant selection models in view of polarity

Variant selection models which have been reviewed before(48, 50, 59), will be described briefly. The MT interacts with external stress because MT has an element of shear deformation. Since each martensite crystal (called variant) transformed from an original austenite crystal is accompanied with a different deformation component (which will be called *"Characteristic Deformation (CD)"* hereafter), the variants are selected to form under the action of stress. The most wellknown concept for *CD* will be the change in external shape, as proposed by J.R. Patel and M. Cohen(60). This has been called *"Shape Deformation (SD)"* model. However, this model has been proved incorrect by detailed TEM study of Y. Higo *et al.*(46).

There were some investigators who considered the deformation by operative slip in austenite as *CD*(61–63). A unique combination of the plane and direction of opera-

Table 10 Variant selection models in the γ to α martensitic transformation

Models	Characteristic Deformation *CD*	Orientation Relation used in Calculation(48, 49)	Polarity of *CD*
SD	Shape deformation	–	?
ASS	Deformation due to dislocations of active slip system in γ	*K-S*	×
BPBR	Deformation due to inactive slip system in γ	*K-S*	×
TS	Twinning shear	*N*	○
BS	Bain strain (lattice deformation)	*Bain*	○

tive slip (*i.e.* for total dislocations) is used to select the *K-S* variants. This model has been called *"Active Slip System (ASS)"* model(48, 50, 59). J.C. Bokros and E.R. Parker(64), on the other hand, found that the normal direction of each martensite habit plane lay close to one of several slip directions of inactive slip system. On this basis, F. Borik and R.H. Richman(65) explained transformation texture and calculated the variants in a similar way to the *ASS* model. This will be called *"Bokros-Parker-Borik-Richman (BPBR)"* model, though it was called *"BP"* model formerly(48, 50, 59). In the *BPBR* model, such variants do not appear that are related with active slip systems. Therefore, variants selected by *BPBR* and *ASS* models are complementary and the two models are incompatible with each other. Besides, in the *ASS* or *BPBR* model polarity is not taken into account because of the use of *K-S* relation. Computer simulation studies of transformation textures were made with these models and compared with experimental textures, but the results revealed the invalidity of the models(48, 50).

Y. Higo *et al.*(46) have adopted the first shear (*i.e.* twinning shear) in the double shear mechanism(6) as *CD*. This has been called *"Twinning Shear (TS)"* model. *N* relation has been proposed convenient in the application of *TS* model(48, 50). The Bain strain has also been regarded as *CD*(47, 48, 50). This has been called *"Bain Strain (BS)"* model. The use of *Bain* relation has been recommended as an effective ways in applying *BS* model(49, 50). The important point is that the polarity has been integrated in these two models, as described in the previous section. With these two models, good matching between experimental data and theoretical predictions have been obtained(46–48, 50). Comparisons among the models are summarized in Table 10.

In conclusion, *BS* and *TS* models in which polarity concept is integrated are successful, but *ASS* and *BPBR* models without taking account the polarity are unsuccessful in explaining the variant selection phenomena.

5. Summary and Conclusion

Conclusions drawn from the above discussion will be summarized as follows.

1) The *RLC* principle is widely applicable in the geometrical plastic properties between bcc and fcc metals, and established properties of a lattice can be used to predict uncertain properties of the reciprocal lattice. Active slip planes in bcc lattice is concluded exclusively as {011} and {112}; the reality of slip on {123} or higher index planes is low.
2) The *SDP* principle is an important nature in understanding the plasticity, including martensitic transformation. The polarity in slip on {112} planes in bcc has been found experimentally as the result of application of the *SDP*.
3) The slip along <001> direction in bcc and the slip on {001} plane in fcc are equally possible.
4) Deformation textures can be estimated from the *RLC*, since the textures are formed as a result of slip deformation.
5) Mechanical twinning and stacking faults in the cubic lattices have been discussed based on the *SDP* and *RLC*. Several geometrical possibilities of stacking faults in bcc are discussed but the presence of stacking faults similar to fcc are not supported.
6) Orientation relationships of martensitic transformation are more or less theoretical, since experimental accuracy to determine the relations does not seem to be high enough for the distinction among them. In this sense *K-S* relation does not represent the *SDP* which is essential in the martensitic transformation.
7) Successful models, *i.e.* *BS* or *TS* models, of variant selection phenomena in martensitic transformation are those in which the *SDP* has been taken into account.

Acknowledgements

This work has been conducted in NRIM, and the author is deeply indebted to many persons in NRIM who have given encouragement and helpful discussions to him. Dr. Kazuyoshi Nii, Director-General of NRIM has been interested in the works and has recommended to apply as the material for publication in NRIM Special Report. The study of slip systems in bcc metals has been conducted under the guidance of Prof. Tadami Taoka, the former Director, Metal Physics Division of NRIM.

Discussions with Profs. Hiroshi Kimura and Shin Takeuchi are very fruitful in constructing the theoretical basis of this volume. Profs. Toru Araki, Tsutomu Mori and Hirosuke Inagaki have given him interest and kind support in developing the variant selection models. He would like to express sincere thanks to all of them.

A. List of Codes

NRIM:	National Research Institute for Metals	(p. 2)
SF:	Stacking Faults	(p. 4)
RLC:	Reciprocal Lattice Correspondence	(p. 2)
MT:	Martensitic Transformation	(p. 4)
SDP:	Shear Deformation Polarity	(p. 4)
BV:	Burgers Vector	(p. 5)
TEM:	Transmission Electron Microscope	(p. 5)
TD:	Total (perfect) Dislocations	(p. 7)
LP:	Leading Partial (dislocations)	(p. 8)
TP:	Trailing Partial (dislocations)	(p. 8)
K-S:	Kurdjumov-Sachs (relation)	(p. 11)
N:	Nishiyama (relation)	(p. 11)
G-T:	Greninger-Troiano (relation)	(p. 11)
CD:	Characteristic Deformation	(p. 11)
SD:	Shape Deformation (model)	(p. 11)
ASS:	Active Slip System (model)	(p. 12)
BPBR:	Bokros-Parker-Borik-Richman (model)	(p. 12)
TS:	Twinning Shear (model)	(p. 12)
BS:	Bain Strain (model)	(p. 12)

References

1) E. Schmid and W. Boas: *Plasticity of Crystals (English translation)* (1950), [F.A. Hughes], 55.
2) W.T. Read, Jr: *Dislocations in Crystals*, (1953), 1.
3) C.S. Barrett and T.B. Massalski: *Structure of Metals, third edition*, (1966), [McGraw-Hill], 1.
4) C.M. Wayman: *Introduction to the Crystallography of Martensitic Transformations*, (1964), [Macmilan], 1.
5) E.C. Bain: Trans. AIME, **70** (1924), 25.
6) A.J. Bogers and W.G. Burgers: Acta Met., **12** (1964), 255.
7) N.K. Chen and R. Maddin: Trans. AIME, **191** (1951), 937.
8) R. Maddin and N.K. Chen: Trans. AIME, **197** (1953), 1131.
9) C.S. Barrett, G. Ansel and R.F. Mehl: Trans ASM, **25** (1937), 702.
10) T. Taoka, S. Takeuchi and E. Furubayashi: J. Phys. Soc. Japan, **19** (1964), 701.
11) S. Takeuchi, E. Furubayashi and T. Taoka: Acta Met., **15** (1967), 1179.
12) S. Takeuchi, H. Yoshida and T. Taoka: Trans. JIM, Suppl. **9** (1968), 715.
13) E. Furubayashi: J. Phys. Soc. Japan, **27** (1969), 130.
14) S. Ikeno and E. Furubayashi: *Phys. Stat. Sol.*;(**a**)**12** (1972), 611.
15) C.S. Barett and T.B. Massalski: p. 404 in the literature 3).
16) E. Furubayashi: unpublished data.
17) S. Takeuchi: unpublished work.
18) W.A. Rachinger and A.H. Cottrell: Acta Met., **4** (1956), 109.
19) E.A. Calnan and C.J.B. Clews: Phil. Mag., **41** (1950), 1085.
20) E.A. Calnan and C.J.B. Clews: Phil. Mag., **42** (1951), 616.
21) Y. Tozawa, M. Nakayama and T. Ishikawa: J. Japan Inst. Tech. Plasticity, **17** (1976), 37.
22) B. Sestak and S. Libovicky: Czech. J. Phys., **B13** (1963), 266.
23) R.A. Foxall, M.S. Duesbery and P.B. Hirsch: Canad. J. Phys., **45** (1967), 607.
24) G. Taylor and J.W. Christian: Phil. Mag., **15** (1967), 873; *ibid.* 893.
25) P.J. Sherwood *et al.*: Canad. J. Phys., **45** (1967), 1075.
26) F. Guiu: Scripta Met., **3** (1969), 449.
27) A.S. Argon and S.R. Maloof: Acta Met., **14** (1966), 1449.
28) P.B. Hirsch: Trans. JIM, Suppl. **9** (1968), XXX.
29) J.W. Christian: Met. Trans., **14A** (1983), 1237.
30) A. Yamamoto *et al.*: J. Japan Inst. Metals, **47** (1983), 903.
31) R. Honda: Bur. Phys. Soc. Japan, **21** (1966), 704.

32) P. Haasen: Phil. Mag., **3** (1958), 384.
33) H. Suzuki and C.S. Barrett: Acta Met., **6** (1958), 156.
34) A. Fourdeux and A. Berghezan: J. Inst. Metals, **89** (1960–61), 31.
35) R. Segall: Acta Met., **9** (1961), 975.
36) A.H. Cottrell and B.A. Bilby: Phil. Mag., **42** (1951), 573.
37) H. Suzuki: *Introduction to Dislocation Theory* (1967) [AGNE] in Japanese, 191.
38) C. Crussard: C.R. Acad. Sci. Paris, **252** (1961), 273.
39) J.B. Cohen, R. Hinton, K. Lay and S. Sass: Acta Met., **10** (1962), 892.
40) C.S. Hartley: Phil. Mag., **14** (1966), 1207.
41) R.H. Richman: *Deformation Twinning* [Gordon & Breach], 237.
42) D.G. Brandon: Acta Met., **14** (1966), 1479.
43) Ch.V. Kopezky *et al.*: Acta Met., **33** (1985), 873.
44) M.S. Wechsler and D.S. Lieberman and T.A. Read: Trans. AIME, **197** (1953), 1503.
45) J.S. Bowles and J.K. Mackenzie: Acta Met., **2** (1954), 129; 138; 224.
46) Y. Higo, F. Lecroisey and T. Mori: Acta Met., **22** (1974), 313.
47) M. Kato and T. Mori: Acta Met., **25** (1977), 951.
48) E. Furubayashi: Tetsu-To-Hagane, **71** (1985), 1155.
49) E. Furubayashi: Tetsu-To-Hagane, **71** (1985), 1359.
50) E. Furubayashi, H. Miyaji and M. Nobuki: Trans. ISIJ, **27** (1987), 513.
51) H. Miyaji *et al.*: Proc. Int. Conf. Physical Metallurgy of Thermomechanical Processing *(THERMEC 88)*[ISIJ], **2** (1988), 815.
52) H. Miyaji and E. Furubayashi: Textures & Microstructures, **22** (1993), 43.
53) G. Kurdjumov and G. Sachs: Z. Phys., **64** (1930), 325.
54) Z. Nishiyama: Sci. Rep. Tohoku Univ., **23** (1934), 637; *ibid.* **25** (1936), 79.
55) W. Pitsch: Arch. Eisenhüttenwes., **30** (1959), 503.
56) A.B. Greninger and A.R. Troiano: Trans. AIME, **185** (1949), 590.
57) E. Furubayashi: Scripta Met. e. Mat., **27** (1992), 1493.
58) Z. Nishiyama, K. Shimizu and K. Sugino: Acta Met., **9** (1961), 620.
59) R.K. Ray and J.J. Jonas: Int. Me. Rev., **35** (1990), 1.
60) J.R. Patel and M. Cohen: Acta Met., **1** (1953), 531.
61) H. Abe and K. Ito: J. Japan Inst. Metals, **31** (1967), 1300.
62) S. Watanabe, T. Araki and H. Miyaji: Trans. ISIJ, Suppl. **11** (1971), 1020.
63) G. Stone and G. Thomas: Met. Trans., **5** (1974), 2095.
64) J.C. Bokros and E.R. Parker; Acta Met., **11** (1963), 1291.
65) F. Borik and R.H. Richman: Trans. AIME, **239** (1967), 675.
66) H. Hu and R.S. Cline: J. Appl. Phys., **32** (1961), 760; *ibid.* 1392.
67) C.G. Dunn and P.K. Koh: Trans. AIME, **203** (1955), 401; *ibid.* **206** (1956), 1017.

A Simple Geometrical Approach to the Prediction of
Plastic Properties of Metal Crystals

by

Ei-ichi FURUBAYASHI

NRIM Special Report
(Research Report)
No. 95-01

Date of issue: 31 March, 1995

Publisher, Contact:
Toshikazu ISHII
Planning Office
National Research Institute for Metals
1–2–1, Sengen, Tsukuba-shi, Ibaraki 305, Japan
Phone: +81-298-53-1045   Fax: +81-298-53-1005

Typeset using the SGML by Uniscope, Inc., Tokyo

A Simple Geometrical Approach to the Prediction of Plastic Properties of Metal Crystals

by

Ei-ichi FURUBAYASHI

NRIM Special Report
(Research Report)
No. 95–01

Contents